Chemical Science

Accepted Manuscript

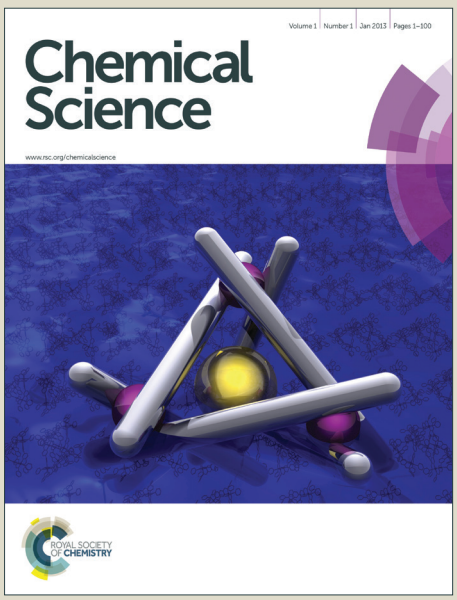

ROYAL SOCIETY OF CHEMISTRY

www.rsc.org/chemicalscience

Chemical Science

RSCPublishing

ARTICLE

Semiconductor-Driven "Turn-Off" Surface-Enhanced Raman Scattering Spectroscopy: Application in Selective Determination of Chromium(VI) in Water

Wei Ji,[a] Yue Wang,[a,b] Ichiro Tanabe,[a] Xiaoxia Han,[b] Bing Zhao,*[b] and Yukihiro Ozaki*[a]

Cite this: DOI: 10.1039/xoxxoooooox

Received ooth January 2012,
Accepted ooth January 2012

DOI: 10.1039/xoxxoooooox

www.rsc.org/

Semiconductor materials have been successfully used as surface-enhanced Raman scattering (SERS)-active substrates, providing the SERS technology with a high flexibility for application in a diverse range of fields. Here, we employ dye-sensitized semiconductor system combined with semiconductor-enhanced Raman spectroscopy to detect metal ions, using an approach based on the "turn-off" SERS strategy that takes advantage of the intrinsic capacity of the semiconductor to catalyze a Raman probe. Alizarin red S (ARS)-sensitized colloidal TiO_2 nanoparticles (NPs) are selected as an example to show how semiconductor-enhanced Raman spectroscopy enables the determination of Cr(VI) in water. Firstly, we explored the SERS mechanism of ARS-TiO_2 complexes and found that the strong electronic coupling between ARS and colloidal TiO_2 NPs gives rise to the formation of a ligand-to-metal charge-transfer (LMCT) transition, providing a new electronic transition pathway for the Raman process. Secondly, colloidal TiO_2 nanoparticles as an active site to induce the self-degradation of the Raman probe adsorbed on its surface in the presence of Cr(VI). Our data demonstrate the potential of ARS-TiO_2 complexes as a SERS-active sensing platform for Cr(VI) in an aqueous solution. Remarkably, the method proposed in this contribution is relatively simple, without requiring complex pretreatment and complicated instruments, but provides high sensitivity and excellent selectivity in a high-throughput fashion. Finally, the ARS-TiO_2 complexes are successfully applied to the detection of Cr(VI) in environmental samples. Thus, the present work provides a facile method for the detection of Cr(VI) in aqueous solutions and a viable application for semiconductor-enhanced Raman spectroscopy based on chemical enhancement contribution.

Introduction

In recent years, an increasing interest in the studies of surface-enhanced Raman scattering (SERS) on semiconducting materials (that is semiconductor-enhanced Raman spectroscopy) has emerged owing to its potential application in biological and photoelectronic analyses.[1-6] Several semiconductor materials including TiO_2, ZnO, graphene, Si, and Ge have been developed as SERS substrates.[7-9] However, the application of these materials in SERS-based quantitative measurements is still matter of debate because of their specific dependence on the molecular electronic structure and relatively weak enhancement contribution to SERS. Most of the semiconductor-enhanced Raman spectroscopy is mainly induced by a charge-transfer process, leading to an enhancement approximately 10^2–10^4, because the surface plasmon resonance of semiconductor NPs typically lies in the infrared region, which does not usually coincide with the optical laser frequency.[2-4, 7-13] To date, studies have largely focused on the discovery and interpretation of the SERS phenomena with different semiconductor materials. This represents the most significant bottleneck in the application of such technique for practical analysis and detection.

The advantage of semiconductor-enhanced Raman spectroscopy is the performance of the semiconductor, which possesses controllable photoelectric properties, good biocompatibility, and environmental stability. In order to exploit these advantages, metal-semiconductor composites were introduced into SERS-based assays with some ingenious designs.[14-19] However, the complicated process need to prepare such composites has strongly limited their application. In addition, semiconductor materials do not respond to the Raman enhancement in these systems.[16-19] Considering the photocatalysis of semiconductor, quantitative analysis by

semiconductor-enhanced Raman spectroscopy would be achieved through the detection of signal degradation of a labeled probe on a semiconductor. Here, we report that semiconductor-enhanced Raman spectroscopy can also be developed into a sensing platform for metal ions detection, even without the assistance of a noble metal. In particular, we present a novel "turn-off" SERS strategy and demonstrate its use in a SERS-based assay for the determination of Cr(VI) in water.

Cr has been extensively used in various industrial processes and has become one of the major environmental hazards.[20] The toxicological and biological properties of Cr are entirely dependent on its electric charge.[21] For instance, Cr(VI) is highly toxic; it generally exists as an oxyanion (CrO_4^{2-}) in aqueous systems, and is known to be a strong carcinogen.[22] In contrast, Cr(III) is relatively non-toxic and is regarded as an essential trace element associated with the metabolism of carbohydrates and lipids.[23] Therefore, the reduction of Cr(VI) to Cr(III) is a key process for the detoxification of Cr(VI)-contaminated water and wastewater. In drinking water, the Maximum Contaminant Level (MCL) for Cr(VI) has been identified as 1 μM. However, because no efficient testing method is available for Cr(VI) only, the estimated MCL by the World Health Organization (WHO) includes the total amount of Cr.[24] Evidently, this definition is not conducive to the intake of Cr(III) from daily diet and has pushed up the cost of industrial wastewater treatment. So far, several methods, including atomic spectrometric,[25-27] luminescent,[28, 29] electrometric,[30-33] colorimetric,[34] and X-ray fluorometric techniques,[35] have been developed for the selective determination of Cr(VI). Nevertheless, none of these techniques exhibited the desired sensitivity together with an easy manipulation.

Herein, facile charge-transfer complexes, alizarin red S (ARS)-sensitized colloidal TiO_2 NPs, are used to demonstrate how semiconductor-enhanced Raman spectroscopy enables the determination of Cr(VI) in water. We explored the SERS mechanism of ARS-TiO_2 complexes and found that the molecular polarizability tensor can be enhanced by a ligand-to-metal charge-transfer (LMCT) transition. Interestingly, SERS intensities of ARS-TiO_2 complexes have been found to be sensitive to Cr(VI) concentration due to a co-catalysis, indicating their potential use in the determination of Cr(VI). Several influencing factors such as response time, laser power, pH of the sensing system, and the loading amount of ARS on colloidal TiO_2 NPs were taken into account to optimize the determination conditions. Our experimental results revealed that the ARS-TiO_2 complexes exhibit high sensitivity and selectivity toward Cr(VI). The practicality of this proposed method was further validated through the detection of Cr(VI) in real water samples. The method proposed here can be used for the determination of Cr(VI) in aqueous solutions for an accurate assessment of pollution levels. Thus, this work provides an evident proof for concept of extending the application of semiconductor-enhanced Raman spectroscopy.

Experimental

Materials: Alizarin red S and titanium (IV) butoxide were acquired from Sigma-Aldrich Co. LTD. and used without further purification. All other chemicals, obtained from Wako Co. LTD, were analytic grade and employed without further purification. Ultrapure water (18 MΩ cm) was used throughout the study. The tap-water and pond-water were collected from Gakuen district of Sanda and a pond near Kwansei Gakuin University, respectively. All the water samples were filtered through 0.2 μm membranes prior to use.

Preparation of colloid TiO_2 nanoparticles: The colloid TiO_2 NPs were synthesized according to a method described in previous reports.[36, 37] Briefly, a solution of titanium (IV) butoxide (5 mL) dissolved in 2-propanol (95 ml) was added dropwise (1 mL/min) to an aqueous HNO_3 solution (500mL, pH 1.5) maintained at 1 ℃. The solution was continuously stirred for 10-12 hours until a transparent colloid was formed.

SERS measurement: A stock solution of ARS (0.1 M) was prepared in water. ARS solutions with various concentrations were obtained by serial dilution of the stock solution with sodium acetate buffer solution (0.01 M, pH 3.0). The ARS solutions with different concentration was mixed with colloid TiO_2 NPs at the same volume and shaken thoroughly. For metal ions detection, 10 μL of each sample mixed with 10 μL of ARS-TiO_2 was dripped into an aluminum pan (0219-0062, Perkin-Elmer), and the mixture was exposed to a laser beam for 30 s before each SERS measurement. The typical exposure time for each Raman/SERS measurement in this study was 30 s with two accumulations. The error bars represent standard deviations based on three independent measurements.

Instrument: The image of sample was measured on a Tecnai G2 transmission electron microscope (TEM) operating at 200 kV. The UV-vis spectra were recorded on a Shimadzu UV-3600 spectrophotometer. A RS-2100 Raman spectrophotometer (Photon Design, Inc.) equipped with a CCD (Princeton Instruments) was used. Radiation with the wavelength of 514.5 nm from an Ar ion laser (Spectra Physics) was employed for the Raman excitation with a power of 5 mW at a sample. The Raman band of the silicon wafer at 520.7 cm^{-1} was used to calibrate the spectrometer.

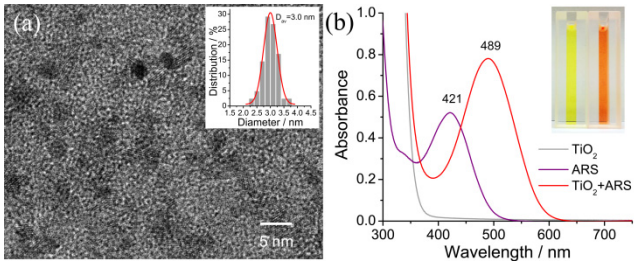

Fig. 1 (a) High-resolution TEM image of colloid TiO_2 nanoparticles. Inset is size distribution of colloid TiO_2 nanoparticles (D_{av} is the average particle size). (b) Optical absorption spectra of colloid TiO_2 nanoparticles (30 mM), ARS (0.1 mM), and ARS-TiO_2 complexes at pH 1.5. The inset shows the corresponding sample photographs.

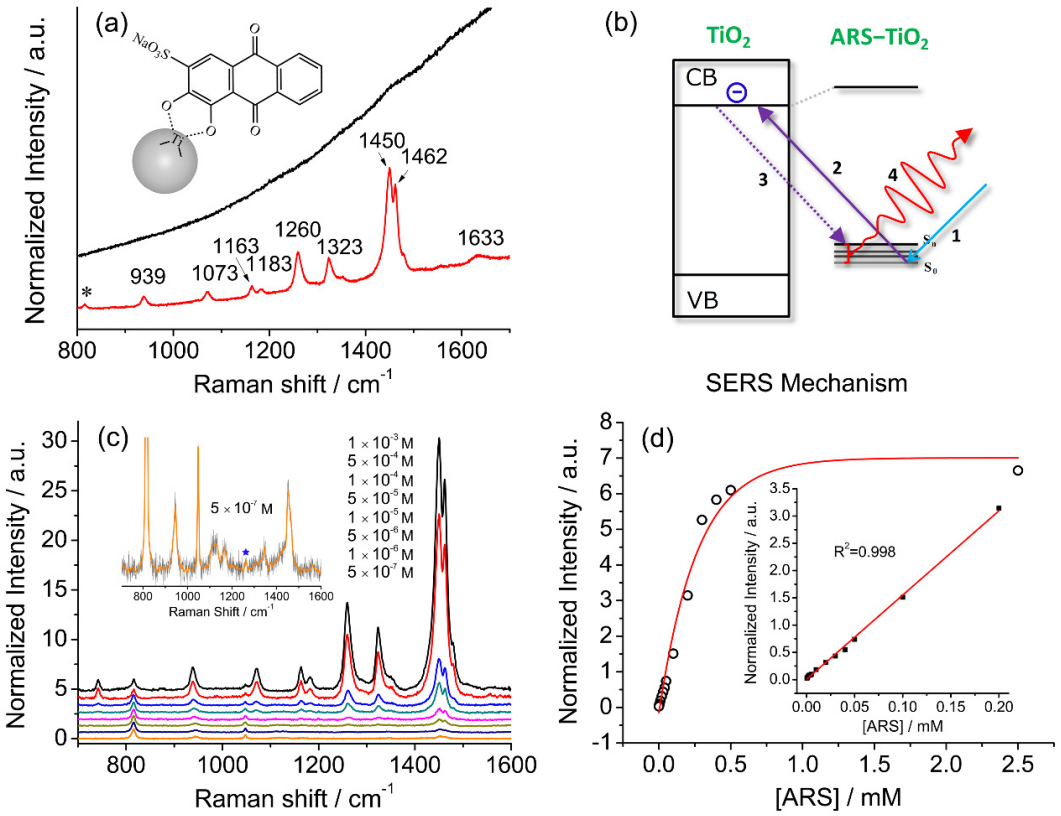

Fig. 2 (a) A Raman spectrum of 0.1 M ARS in aqueous solution (top) and a SERS spectrum of 10^{-3} M ARS adsorbed on colloid TiO_2 NPs (bottom). (b) Suggested mechanism for the photoexcitation charge-transfer process of ARS-TiO_2 complexes with 514.5 nm excitation. (c) SERS spectra of ARS with variable concentrations adsorbed on colloid TiO_2 NPs. Inset: the magnified SERS spectrum of ARS-TiO_2 under 5×10^{-7} M. (d) Normalized Raman intensity at 1260 cm^{-1} versus the concentration of ARS. Inset represents low concentration. All the intensities of the bands are normalized to the intensity of the signal due to 2-propanol at 816 cm^{-1}.

Results and discussion

Synthesis and Characterization

Colloidal TiO_2 NPs with an average diameter of 3 nm were prepared by a low-temperature acid hydrolysis route, as described previously (see Fig. 1).[36, 37] The absorption spectra of colloidal TiO_2 NPs before and after modification with ARS are shown in Fig. 1b, together with that of ARS for the sake of comparison. In contrast to ARS, the ARS-TiO_2 complexes exhibit a more intense absorption band in the longer wavelength region with a peak maximum centered at 489 nm. This absorption band has been assigned to the LMCT transition, which arises from the strong electronic coupling between ARS and the colloidal TiO_2 NPs.[38] Based on the Benesi-Hildebrand analysis for ARS-TiO_2 complexes (Fig. S1†), the association constant (K_{ass}) of the complex was determined to be 3.9×10^3 M^{-1}, which indicates a relatively strong binding of ARS on the surface of TiO_2 NPs. An ARS molecule contains many functional groups, the FTIR data of ARS-TiO_2 complexes unambiguously shows that the mode of grafting is bidentate chelation, which involves two hydroxyl groups (Fig. S2†). These observations suggest that the ARS-TiO_2 composite material can be used for the development of a semiconductor-supported SERS sensing platform due to their clear charge-transfer transition process.

Mechanism for SERS of ARS-TiO_2 system

Fig. 2a compares a Raman spectrum of 0.1 M ARS in aqueous solution and a SERS spectrum of ARS-TiO_2 complexes with the 514.5 nm excitation. The vibrational mode assignments listed in Table S1 are based primarily on earlier IR and Raman studies of related alizarin dyes.[39-42] The SERS spectrum is characterized by a significant enhancement in the 1200–1500 cm^{-1} region, where the bands are typically assigned to the C=C and C-O-R stretching modes. This observation confirms that the presence of strong coupling between the electronic transition and the C=C/C-O-R bond stretching modes in ARS ligands, which are consistent with the conclusions obtained from the absorption and IR spectra of ARS-TiO_2 complexes. Such coupling has also been observed on other semiconductor NPs in colloidal suspensions such as CeO_2, Fe_2O_3, ZrO_2, etc.[43] Furthermore, the concentration-dependent SERS experiments displayed in Fig. 2c clearly demonstrate that the concentration as low as 5×10^{-7} M ARS can be detected.[44] The intensities of the Raman signals can be well fit with the BET model and represent a saturate effect (Fig. 2d). In addition,

a linear correlation was found between the intensity at 1260 cm^{-1} and the ARS concentration in the range of 5×10^{-7}- 2×10^{-4} M.

Of note is that the enhancement arises from the strong coupling interaction between the dye molecules and the colloidal TiO_2 NPs and, more importantly, the formation of charge-transfer complexes opens up a new electronic transition pathway for the Raman process.[45, 46] In this case, the ground-state electrons of the ARS-TiO_2 complexes are initially excited from the highest occupied molecular orbital (HOMO) level to the conduction band (CB) of TiO_2 NPs by incident light (Fig. 2b). Then, the excited electrons immediately transfer back to the vibrational energy level of the ARS molecule and subsequently release a Raman photon with the ARS molecule at some vibrational state. The molecular polarizability tensor can be enhanced by such charge transfer process due to the vibronic coupling of the conduction band states of the semiconductor with the excited states of the probe molecule through a Herzberg-Teller coupling term.[47] Therefore, unlike the resonance Raman where the molecule itself should reach a resonance state with the excitation of incident light, the enhancement can be considered in this case as a SERS phenomenon which arises from the chemical enhancement mechanism via the Herzberg-Teller contribution.[2, 45, 48]

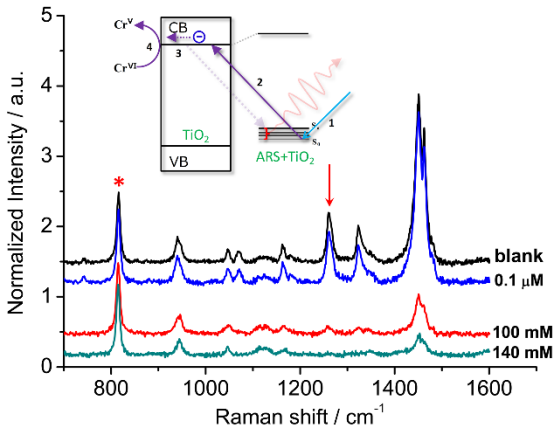

Fig. 3 SERS spectra observed from the ARS-TiO_2 (50 μM ARS) mixtures with the various Cr(VI) concentrations. The intensities of the bands are normalized to that of the signal from 2-propanol at 816 cm^{-1}. Inset: suggested mechanism for the photoexcitation catalysis process of ARS-TiO_2 complexes in the presence of Cr(VI).

Mechanism for responding to Cr(VI)

In general, organic ligands are susceptible to decompose on bulk TiO_2, owing to their adsorption through physisorption or weak chemisorption. Compared with bulk TiO_2, colloidal TiO_2 NPs possess abundant under-coordinated Ti defect sites, which provide plenty of coordination sites for ARS to bind via a bidentate chelation. This chelation mode is favorable to the recombination between ARS^+ and electron, thereby stabilizing the ARS molecule. Consequently, ARS adsorbed on the surface of colloidal TiO_2 NPs cannot be easily oxidized by visible light irradiation and preserves the SERS property even after exposure to high laser power (Fig. S4†). However, SERS intensities are decreased with the addition of Cr(VI), indicating the decomposition of ARS adsorbed on the colloidal TiO_2 NPs surface (Fig. 3 and Fig. S5†). As shown in Fig. 4 and Fig. S6†, the ARS-TiO_2 complexes exhibit a remarkably high selectivity and lower interference toward Cr(VI), particularly in the presence of Cr(III). This specificity originates from the favorable redox potential of the couple Cr(VI)/Cr(V) (+0.55 V) for the reduction promoted by those electrons trapped in inter-band-gap states, together with the strong interaction between Cr(VI) and Ti(IV) atoms with unfilled valence at the TiO_2 surface. This reduction can result in the formation of Cr(V) and decomposition of ARS-TiO_2 complexes (Fig. S5†), thus leading to a decrease in the SERS intensities. The redox potential of the Fe(III)/Fe(II) couple (+0.77) is close to that of the Cr(VI)/Cr(V) couple. However, the relatively weak interaction between Fe(III) and the positively charged colloidal TiO_2 NPs only causes minor disturbance. To minimize the interference from Fe(III), 0.2 mM EDTA was added to the sodium acetate buffer as a masking agent. As expected, the interference from Fe(III) was found to be negligible in the presence of EDTA. Based on these results, it was inferred that the SERS intensities of ARS are sensitive to the Cr(VI) concentration, indicating the possibility of Cr(VI) detection using ARS-sensitized colloidal TiO_2 NPs.

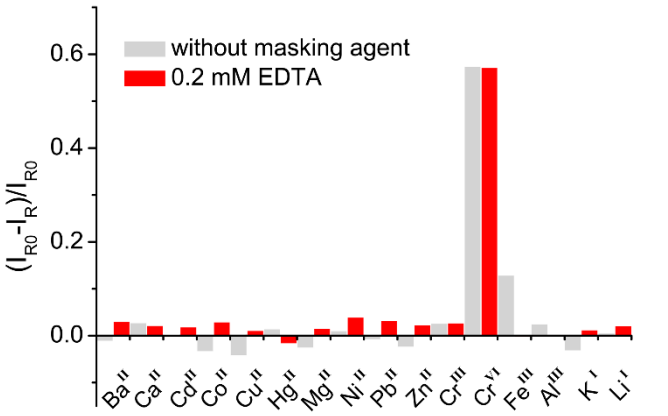

Fig. 4 Relative Raman intensity $[(I_{R0}-I_R)/I_{R0}]$ of ARS-TiO_2 complexes in the presence of metal ions with and without the addition of a masking reagent. The concentration of Cr(VI) was 20μM and each of the other metal ions was 100 μM. I_R and I_{R0} represent the Raman intensities of ARS-TiO_2 at 1260 cm^{-1} in the presence and absence of metal ions, respectively.

Optimization of the Sensing System

Prior to application of such SERS sensing platform to the detection of Cr(VI), several influencing factors such as response time, laser power, pH of the sensing system, and the loading amount of ARS on colloidal TiO_2 NPs must be considered. Firstly, the Cr(VI) induced SERS decrease was found to be fast and reached an equilibrium within 30 s (Fig. S7†), and thus the mixture was exposed to a laser beam for 30s before each SERS measurement. This fast sample preparation is beneficial for high-throughput Cr(VI) assays. Secondly, we compared the affinity of Cr(VI) to colloidal TiO_2 NPs surface in different pH, because acidity affects the surface charge of the colloidal TiO_2 NPs and the existing species of Cr(VI). As shown in Fig. S8†, no changes in the SERS intensities were

observed with pH ranging from 2.0 to 5.0. Within this range, $HCrO_4^-$ is the major Cr(VI) species in the sensing system. Meanwhile, the colloidal TiO_2 surface is positively charged, which is favored to the adsorption of negatively charged ions such as $HCrO_4^-$, CrO_4^{2-}, and $Cr_2O_7^{2-}$. Moreover, an aggregation-sedimentation phenomenon was observed at the pH larger than 5.0, providing us a simple method to recycle the TiO_2 NPs from the analyte. Finally, the response mechanism was based on a co-catalysis scheme, in which both Cr(VI) and ARS are activated by the available Ti-coordination sites on the surface of the colloidal TiO_2 NPs. Thus, the catalytic efficiency with different loading amount of ARS on the colloidal TiO_2 NPs was also conducted to determine the optimum ARS-sensitized concentration. It was clearly found that increasing the loading amount of ARS represents an increase in the SERS intensity, but the best performance was obtained at 50 μM (Fig. S9†).

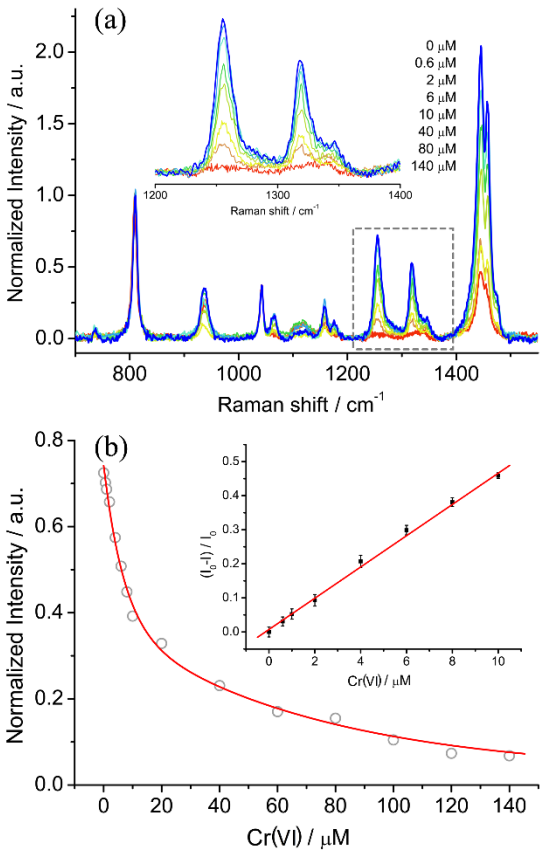

Fig. 5 (a) SERS spectra of ARS-TiO_2 complexes (50 μM ARS) in the absence and presence of Cr(VI) with different concentrations. The intensities of the bands are normalized to that of the signal from 2-propanol at 816 cm^{-1}. (b) The normalized Raman intensity at 1260 cm^{-1} versus the Cr(VI) concentration. The inset shows the relative Raman intensity $[(I_{R0}-I_R)/I_{R0}]$ in the low concentration range.

Application

Based on the optimized conditions, the sensitivity and linearity of this sensing system were evaluated with different concentrations of Cr(VI) (Fig. 5). A good inverse proportionality was observed between the SERS intensity and the amount of Cr(VI) in the concentration range 0.6–10 μM. The lowest concentration, in which Cr(VI) could be detected, is 0.6 μM. This concentration is lower than the maximum level of Cr(VI) in drinking water allowed by the WHO. In addition, the water samples spiked with different concentrations of Cr(VI) were also determined by employing our sensing system (Fig. 6). The measurements, during which the added standard Cr(VI) was accurately measured with good recoveries (Table S2†), confirmed that the sensing system proposed in this work has great potential for the quantitative analysis of Cr(VI) in environmental samples.

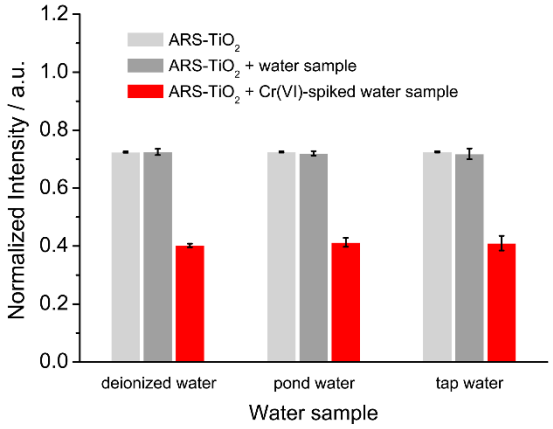

Fig. 6. SERS response of ARS-TiO_2 to different water samples and water samples spiked with 10μM Cr(VI) at pH 3.

Conclusions

In this work, we showed that semiconductor-enhanced Raman spectroscopy can be used as a sensing platform for the detection of metal ions. Firstly, the possibility of utilizing the dye sensitized TiO_2 system to promote SERS is discussed. It is found that the strong coupling interaction between the dye molecules and the colloidal TiO_2 NPs leads to the formation of charge-transfer complexes and thus opens up a new electronic transition pathway for charge transfer process. The molecular polarizability tensor can be enhanced by such charge transfer process due to the vibronic coupling of the conduction band states of the semiconductor with the excited states of the probe molecule through a Herzberg-Teller coupling term. Secondly, a novel "turn-off" SERS strategy has been proposed and its use in a SERS-based assay for Cr(VI) has been demonstrated. Colloidal TiO_2 NPs can be employed not only as an effective substrate to achieve SERS signal of ARS molecule, but also as a catalytic center to induce the self-degradation of the ARS response to Cr(VI). The "turn off" SERS signal upon laser irradiation allows the development of a facile assay to measure Cr(VI). Of note is that this method does not require complex pretreatment and complicated instruments, but provides a high sensitivity in a high-throughput fashion and excellent selectivity toward Cr(VI) over other common anions. Furthermore, spiked experiments revealed that our method is effective in monitoring the Cr(VI) in real water samples. Based on this "turn-off" SERS strategy, other metal ions can also be

detected by utilize different semiconductor enhancement system that the energy level of semiconductor is match with redox potential of determined metal ion. Thus, we believe that the date described in this contribution clearly demonstrate that the semiconductor-enhanced Raman spectroscopy integrated with the catalysis of semiconductor materials can be used as a reliable detection method for metal ions in practical applications.

Acknowledgements

This work was supported by a Support Project to Assist Private Universities in Developing Bases for Research (Research Centre for Single Molecule Vibrational Spectroscopy) from the Ministry of Education, Culture, Sports, Science and Technology of Japan. We are grateful to Dr Tamitake Itoh (National Institute of Advanced Industrial Science and Technology, Japan) for helpful discussions. W. J. acknowledges the support from the Japanese Society for Promotion of Science (JSPS, P13332).

Notes and references

[a] Department of Chemistry, School of Science and Technology, Kwansei Gakuin University, Sanda, Hyogo 669-1337, Japan. E-mail: ozaki@kwansei.ac.jp;

[b] State Key Laboratory of Supramolecular Structure and Materials, Jilin University, Changchun 130012, P. R. China. E-mail: zhaob@mail.jlu.edu.cn;

† Electronic Supplementary Information (ESI) available: Detailed Benesi-Hildebrand plot, IR spectra, Raman assignments, and experiment optimization. See DOI: 10.1039/b000000x/

1. L. G. Quagliano, *J. Am. Chem. Soc.*, 2004, **126**, 7393-7398.
2. A. Musumeci, D. Gosztola, T. Schiller, N. M. Dimitrijevic, V. Mujica, D. Martin and T. Rajh, *J. Am. Chem. Soc.*, 2009, **131**, 6040-6041.
3. X. Ling, L. M. Xie, Y. Fang, H. Xu, H. L. Zhang, J. Kong, M. S. Dresselhaus, J. Zhang and Z. F. Liu, *Nano Lett.*, 2010, **10**, 553-561.
4. X. Wang, W. Shi, G. She and L. Mu, *J. Am. Chem. Soc.*, 2011, **133**, 16518-16523.
5. C. Qiu, L. Zhang, H. Wang and C. Jiang, *J. Phys. Chem. Lett.*, 2012, **3**, 651-657.
6. I. Alessandri, *J. Am. Chem. Soc.*, 2013, **135**, 5541-5544.
7. L. B. Yang, X. Jiang, W. D. Ruan, B. Zhao, W. Q. Xu and J. R. Lombardi, *J. Phys. Chem. C*, 2008, **112**, 20095-20098.
8. Y. F. Wang, W. D. Ruan, J. H. Zhang, B. Yang, W. Q. Xu, B. Zhao and J. R. Lombardi, *J. Raman Spectrosc.*, 2009, **40**, 1072-1077.
9. X. Wang, W. Shi, G. She and L. Mu, *Phys. Chem. Chem. Phys.*, 2012, **14**, 5891-5901.
10. D. Finkelstein-Shapiro, P. Tarakeshwar, T. Rajh and V. Mujica, *J. Phys. Chem. B*, 2010, **114**, 14642-14645.
11. S. Ma, R. Livingstone, B. Zhao and J. R. Lombardi, *J. Phys. Chem. Lett.*, 2011, **2**, 671-674.
12. X. X. Xue, W. Ji, Z. Mao, H. J. Mao, Y. Wang, X. Wang, W. D. Ruan, B. Zhao and J. R. Lombardi, *J. Phys. Chem. C*, 2012, **116**, 8792-8797.
13. J. R. Lombardi and R. L. Birke, *J. Phys. Chem. C*, 2014, **118**, 11120-11130.
14. W. Ji, X. X. Xue, W. D. Ruan, C. X. Wang, N. Ji, L. Chen, Z. S. Li, W. Song, B. Zhao and J. R. Lombardi, *Chem. Commun.*, 2011, **47**, 2426-2428.
15. W. Ji, Y. Kitahama, X. X. Han, X. X. Xue, Y. Ozaki and B. Zhao, *J. Phys. Chem. C*, 2012, **116**, 24829-24836.
16. X. H. Li, G. Y. Chen, L. B. Yang, Z. Jin and J. H. Liu, *Adv. Funct. Mater.*, 2010, **20**, 2815-2824.
17. W. Xu, X. Ling, J. Xiao, M. S. Dresselhaus, J. Kong, H. Xu, Z. Liu and J. Zhang, *Proc. Natl. Acad. Sci. USA*, 2012, **109**, 9281-9286.
18. C. Wen, F. Liao, S. Liu, Y. Zhao, Z. Kang, X. Zhang and M. Shao, *Chem. Commun.*, 2013, **49**, 3049-3051.
19. X. X. Han, L. Chen, U. Kuhlmann, C. Schulz, I. M. Weidinger and P. Hildebrandt, *Angew. Chem. Int. Edit.*, 2014, **53,** 2481-2484.
20. S. M. Booker and C. Pellerin, *Environ. Health Perspect.*, 2000, **108**, 402-407.
21. S. A. Katz and H. Salem, *J. Appl. Toxicol.*, 1993, **13**, 217-224.
22. R. Saha, R. Nandi and B. Saha, *J. Coord. Chem.*, 2011, **64**, 1782-1806.
23. J. B. Vincent, *Acc. Chem. Res.*, 2000, **33**, 503-510.
24. Guidelines for Drinking-Water Quality, 4th ed, World Health Organization, 2011. Also available at http://www.who.int/water_sanitation_health/publications/2011/dwq_guidelines/en/ (accessed March 2014).
25. M. Sperling, S. Xu and B. Welz, *Anal. Chem.*, 1992, **64**, 3101-3108.
26. X. Zhang and J. A. Koropchak, *Anal. Chem.*, 1999, **71**, 3046-3053.
27. M. Gardner and S. Comber, *Analyst*, 2002, **127**, 153-156.
28. D. F. Marino and J. D. Ingle, *Anal. Chem.*, 1981, **53**, 294-298.
29. H. Q. Chen and J. C. Ren, *Talanta*, 2012, **99**, 404-408.
30. L. Yong, K. C. Armstrong, R. N. Dansby-Sparks, N. A. Carrington, J. Q. Chambers and Z.-L. Xue, *Anal. Chem.*, 2006, **78**, 7582-7587.
31. G. Liu, Y.-Y. Lin, H. Wu and Y. Lin, *Environ. Sci. Technol.*, 2007, **41**, 8129-8134.
32. W. Jin, G. Wu and A. Chen, *Analyst*, 2014, **139**, 235-241.
33. B. K. Jena and C. R. Raj, *Talanta*, 2008, **76**, 161-165.
34. X. Y. Wu, Y. B. Xu, Y. J. Dong, X. Jiang and N. N. Zhu, *Anal. Methods*, 2013, **5**, 560-565.
35. I. Tsuyumoto and Y. Maruyama, *Anal. Chem.*, 2011, **83**, 7566-7569.
36. D. Bahnemann, A. Henglein, J. Lilie and L. Spanhel, *J. Phys. Chem.*, 1984, **88**, 709-711.
37. H. N. Ghosh, *J. Phys. Chem. B*, 1999, **103**, 10382-10387.
38. Y. D. Iorio, E. S. Román, M. I. Litter and M. a. A. Grela, *J. Phys. Chem. C*, 2008, **112**, 16532-16538.
39. L. C. T. Shoute and G. R. Loppnow, *J. Chem. Phys.*, 2002, **117**, 842-850.
40. D. Pan, D. Hu and H. P. Lu, *J. Phys. Chem. B*, 2005, **109**, 16390-16395.
41. P. M. Jayaweera and T. A. U. Jayarathne, *Surf. Sci.*, 2006, **600**, L297-L300.
42. M. L. de Souza and P. Corio, *Vib. Spectrosc.*, 2010, **54**, 137-141.
43. S. J. Hurst, H. C. Fry, D. J. Gosztola and T. Rajh, *J. Phys. Chem. C*, 2011, **115**, 620-630.
44. The lowest concentration to quantify ARS could be further down through turning the size of colloidal TiO_2 NPs. In general, decreasing the particle size increases the amount of under-coordinated Ti defect

sites and subsequently increases the amount of probe molecules adsorbed on a particle surface. Thus, the enhancement effects will increase with decreasing particle size. However, when the particle size reached its Bohr radius region (for TiO_2 is 1.5 nm), the enhancement effects may plummet due to the quantization effects. The quantization effects will result in select discrete allowed levels from the conduction and valence band continuum, thus decreasing the chemical enhancement borrowed from the allowed transitions within continuum states through Herzberg-Teller vibronic coupling.

45. P. C. Redfern, P. Zapol, L. A. Curtiss, T. Rajh and M. C. Thurnauer, *J. Phys. Chem. B*, 2003, **107**, 11419-11427.
46. R. Huber, S. Spörlein, J. E. Moser, M. Grätzel and J. Wachtveitl, *J. Phys. Chem. B*, 2000, **104**, 8995-9003.
47. The evaluation of vibronic coupling usually involves a complex mathematical treatment. Actually, the direct calculation of vibronic couplings has been very limited so far. For SERS theory, a matrix elements (Herzberg-Teller coupling term) is introduced into the coupling system and represents the vibronic mixing of semiconductor states with molecular states.
48. J. R. Lombardi and R. L. Birke, *Acc.. Chem. Res.*, 2009, **42**, 734-742.